In Vitro Models of Tail Contraction and Cytoplasmic Streaming in Amoeboid Cells

Lee W. Janson and D. Lansing Taylor

Center for Light Microscope Imaging and Biotechnology and Department of Biological Sciences, Carnegie Mellon University, Pittsburgh, Pennsylvania 15213

Abstract. We have developed a reconstituted gel-sol and contractile model system that mimics the structure and dynamics found at the ectoplasm/endoplasm interface in the tails of many amoeboid cells. We tested the role of gel-sol transformations of the actin-based cytoskeleton in the regulation of contraction and in the generation of endoplasm from ectoplasm. In a model system with fully phosphorylated myosin II, we demonstrated that either decreasing the actin filament length distribution or decreasing the extent of actin filament cross-linking initiated both a weakening of the gel strength and contraction. However, streaming of the solated gel components occurred only under conditions where the length distribution of actin was decreased, causing a self-destruct process of continued solation and contraction of the gel. These results offer significant support that gel strength plays an important role in the regulation of actin/myosin II-based contractions of the tail cortex in many amoeboid cells as defined by the solation-contraction coupling hypothesis (Taylor, D. L., and M. Fechheimer. 1982. *Phil. Trans. Soc. Lond. B.* 299:185–197). The competing processes of solation and contraction of the gel would appear to be mutually exclusive. However, it is the temporal-spatial balance of the rate and extent of two stages of solation, coupled to contraction, that can explain the conversion of gelled ectoplasm in the tail to a solated endoplasm within the same small volume, generation of a force for the retraction of tails, maintenance of cell polarity, and creation of a positive hydrostatic pressure to push against the newly formed endoplasm. The mechanism of solation-contraction of cortical cytoplasm may be a general component of the normal movement of a variety of amoeboid cells and may also be a component of other contractile events such as cytokinesis.

One of the most dramatic examples of cell movement is seen in the integration of pseudopod formation, cytoplasmic streaming, and tail retraction exhibited by free-living amoebae, peripheral monocytes, and cellular slime molds (for review see Taylor and Condeelis, 1979). The cytoplasm cycles from a less gelled state (endoplasm), streaming forward from the tail to the tips of extending pseudopods at rates up to 40 μm/s in some cells, to a more gelled state (ectoplasm) as the endoplasm transforms to ectoplasm at the tips of extending pseudopods. The ectoplasm transports toward the rear of the cell where a combination of solation and contraction in a zone of elevated free Ca^{2+} (see Taylor et al., 1980*a*,*b*; Brundage et al., 1991; Hahn et al., 1993; Gough and Taylor, 1993) transforms the ectoplasm back into endoplasm. The mechanism of amoeboid movement can be described as involving the integration of at least three processes that involve ectoplasm and endoplasm conversions: (*a*) the extension of pseudopods; (*b*) the transport of cytoskeletal components into pseudopods; and (*c*) the retraction of the tails.

Please address all correspondence to Dr. Lee W. Janson, NASA-Johnson Space Center, Mail Code SD4, Houston, TX 77058.

Extension of pseudopods is believed to involve one or more of a variety of forces including actin assembly (Abercrombie, 1980; Tilney and Inoue, 1985; Wang, 1985; Fisher et al., 1988; DeBiasio et al., 1988; Smith, 1988; Theriot and Mitchison, 1991), gel expansion (Oster and Perelson, 1987; Stossel, 1990; Condeelis, 1992), osmotic pressure (Oster and Perelson, 1987), positive hydrostatic pressure (Pantin, 1923; Grebecki, 1982; Komnick et al., 1973; Taylor et al., 1980*a*,*b*; Wang et al., 1982), and frontal contraction of endoplasm (Allen, 1973). Recently, the forces involved in pseudopod extension have been the focus of a great deal of attention due to the discovery that amoeboid cells continue to locomote, albeit in an abnormal way, even after the deletion or inhibition of expression of myosin II heavy chains (DeLozanne and Spudich, 1987; Knecht and Loomis, 1987; Wessels et al., 1988) or the microinjection of anti-myosin II antibodies (Honer et al., 1988). Normal translocation of cells must also involve the transport of cytoplasm (endoplasm) into pseudopods and the retraction of the tails. These latter two processes have been described as based on either positive hydrostatic pressure caused by a tail contraction (Pantin, 1923; Taylor et al., 1980 *a*,*b*; Taylor and Fechheimer, 1982) or by a frontal contraction of endoplasm that

transmits the tension posteriorly and causes the passive retraction of the tail (Allen, 1973).

The solation-contraction coupling hypothesis suggests a mechanism for the conversion of ectoplasm to endoplasm and the generation of a force that could both retract the tail and apply a positive hydrostatic pressure that could help deliver subunits of the gel structure forward to the extending pseudopods (Taylor et al., 1980 *a*,*b*; Taylor and Fechheimer, 1982; Conrad et al., 1993). Operational definitions of the classical colloidal chemical terms gel and sol (Taylor and Condeelis, 1979) are required to understand the functional implications of the solation-contraction coupling hypothesis in terms of actin, actin-binding proteins, and molecular motors. *Gel*: An "infinite" network of cross-linked actin filaments that can resist contraction by myosin motors due to the counterforces of the gel including elastic and osmotic forces. The *Gel Point* is a sharp transition when the actin filaments are just cross-linked into an infinite network. *Sol*: A fluid consisting of the subunits of actin, actin-binding proteins, and myosin motors which may include a partially cross-linked network that is below the gel point based on Flory theory (see Flory, 1941; Stossel, 1982).

Flory theory states that the actin gel can be transformed into a sol by either decreasing the number of cross-links (e.g., actin-cross-linking proteins) and/or by decreasing the length distribution of the polymer (e.g., gelsolin severing of actin filaments) in the presence of a fixed number of cross-links. The process of "Solation" can involve two separate stages: (*a*) When the gel is initially cross-linked more extensively than the minimum gel point, restricting the length distribution of *some* actin filaments and/or inhibiting the cross-linking of *some* of the cross-links could decrease the gel strength, while still maintaining the infinite network. This may be termed "partial solation" and could be a gradual process, depending on the initial gel strength. (*b*) Continued solation would ultimately bring the gel structure below the gel point and the whole system would become a sol. This "complete solation" is a sharp transition.

Therefore, a continuum of gel structure can be generated from a maximally gelled state to a fluid sol by regulating the activity of actin cross-linking proteins (e.g., filamin, α-actinin) as well as proteins that regulate the length distribution of actin filaments (e.g., gelsolin). When the strength of the gel is equal to or greater than the forces applied by the myosin motors, only an isometric contraction can occur, no filaments are transported and no work is performed (Fig. 1 *A*). When solation activity decreases the strength of the gel, while maintaining the infinite network (partial solation), the counterforces of the gel can be decreased to the point where the force of the myosin motors can cause an isotonic contraction, resulting in transport of filaments and the performance of work (Fig. 1 *B*). It is important to note that myosin motors are also cross-linkers and the infinite network can be transformed from a predominantly static, cross-linked gel (e.g., filamin) to a predominantly active, cross-linked gel (myosin motors). When the structure of the gel is reduced below the gel point (complete solation), myosin motor force cannot be transmitted through the network and no contractions can occur (Fig. 1 *C*). By balancing the site, rate, extent, and molecular basis of solation, contraction of a continuously weakening gel can culminate in the complete destruction of the contracting network. This sequence of

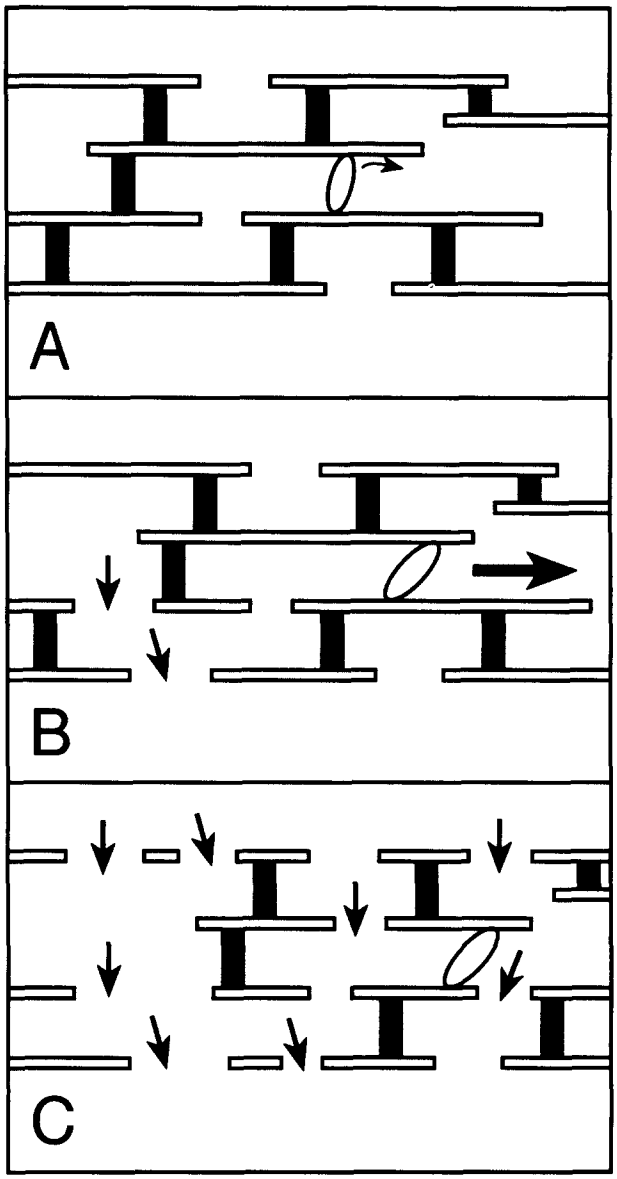

Figure 1. Diagrams depicting the structure of actin-based gels. Rods represent actin filaments, solid bars represent actin-binding proteins that cross-link actin such as filamin, while the tilted ellipses represent myosin motors. Only solation by shortening actin filament lengths is shown for simplicity and to emphasize the self-destruct nature of this solation process. (*A*) Actin-based gel with the maximal gel strength. The myosin motor is exerting isometric tension on the gel, but the heavily cross-linked gel resists the contractile force and actin filaments do not move. (*B*) Activation of proteins that restrict the length of some actin filaments (e.g., gelsolin) on the left side of the diagram cause the shortening of some of the actin filaments (*small arrows*). This first stage of solation (*partial solation*) maintains the infinite network, but decreases the gel strength. The loss of some of the counterforces in the gel permits the myosin motor to do work on the partially solated gel and a contraction is initiated at the site of the first stage of solation. The forces of the contraction work against the gel of greater strength to the right side of the diagram and movement of the network is to the right (*large solid arrow*). (*C*) Solation of the gel below the gel point (*complete solation*) by restricting the length of many of the actin filaments would inhibit contraction (*small arrows*). However, balancing the rate and extent of solation through stages one and two with the rate of motor activity can regulate this self-destruct force generating activity.

events can create a self-destruct contraction mechanism that results in the loss of mass from the contracting network. This concept is the basis of the solation-contraction coupling hypothesis (see Taylor and Fechheimer, 1982), has implications for the mechanisms of all actin-based motors, and probably works in concert with the activation of the motors (Janson et al., 1991; Kolega et al., 1991).

The transformation of the gelled ectoplasm into the solated endoplasm, which is then transported forward out of the tails of many locomoting amoeboid cells, makes this an ideal system to model in vitro. To understand the forces involved in amoeboid movement, we have studied the relationship between gel structure and contraction in a reconstituted system (Janson et al., 1991), a single filament motility assay (Janson et al., 1992), and in living cells (Kolega et al., 1991). Solation and contraction of the reconstituted system, after applying a gradient of cytochalasin D, resulted in both contraction and streaming dynamics similar to that observed in the tails of living cells and in single cell models (Janson et al., 1991; Taylor et al., 1973; Taylor and Fechheimer, 1982). Although these previous studies provided strong evidence suggesting a possible role of gel structure in the regulation of cell motility, the results relied on comparison of static samples or non-physiological methods of solation.

We now present results in which a gradient of solation is produced using two independent methods of solation, calcium-activated restriction of actin filament lengths by gelsolin and inhibition of α-actinin cross-linking by calcium. These methods provide solation by physiological mechanisms free of any possible artifacts from cytochalasin and allow the direct comparison of different gel states and contraction rates in the same sample. This model system mimics the elevation of free calcium in the tails of locomoting free-living amoebae (Taylor et al., 1980*b*), newt eosinophils (Brundage et al., 1991), and fibroblasts (Hahn et al., 1992; Gough and Taylor, 1993), allowing the study of the contraction of ectoplasm, the transition from ectoplasm to endoplasm, the streaming of endoplasm, and the retraction of tails.

Materials and Methods

The Two Model Systems

Two separate model systems were prepared: (*1*) gelsolin samples containing actin, the calcium-independent fragment of gelsolin (Fx-45)[1] for initial actin filament length control, gelsolin, fully phosphorylated myosin II, and filamin; (*2*) α-actinin samples containing actin, Fx-45 for initial actin filament length control, α-actinin, fully phosphorylated myosin II, and filamin. The use of Fx-45 permitted the regulation of actin filament lengths while still maintaining the ability to use a calcium-regulated solating agent (either calcium-regulated gelsolin or calcium-regulated α-actinin) as the major modifier of gel structure. Initially, gelsolin activity was inhibited or α-actinin cross-linking was maintained throughout the reconstitution procedure with 0.11–5 mM EGTA ($<10^{-12}$ M free calcium) (Robertson and Potter, 1984). Addition of calcium to gelsolin samples activated gelsolin and caused partial solation by restricting the lengths of actin filaments which would ultimately cause a loss of mass in the solating gel. Calcium added to α-actinin samples inhibited α-actinin activity, causing partial solation by a decrease in actin filament cross-linking, while maintaining the length distribution of the actin filaments and the cross-linking by filamin.

1. *Abbreviations used in this paper*: Fx-45, calcium-independent fragment of gelsolin; IMLCK, calcium-independent fragment of myosin light chain kinase.

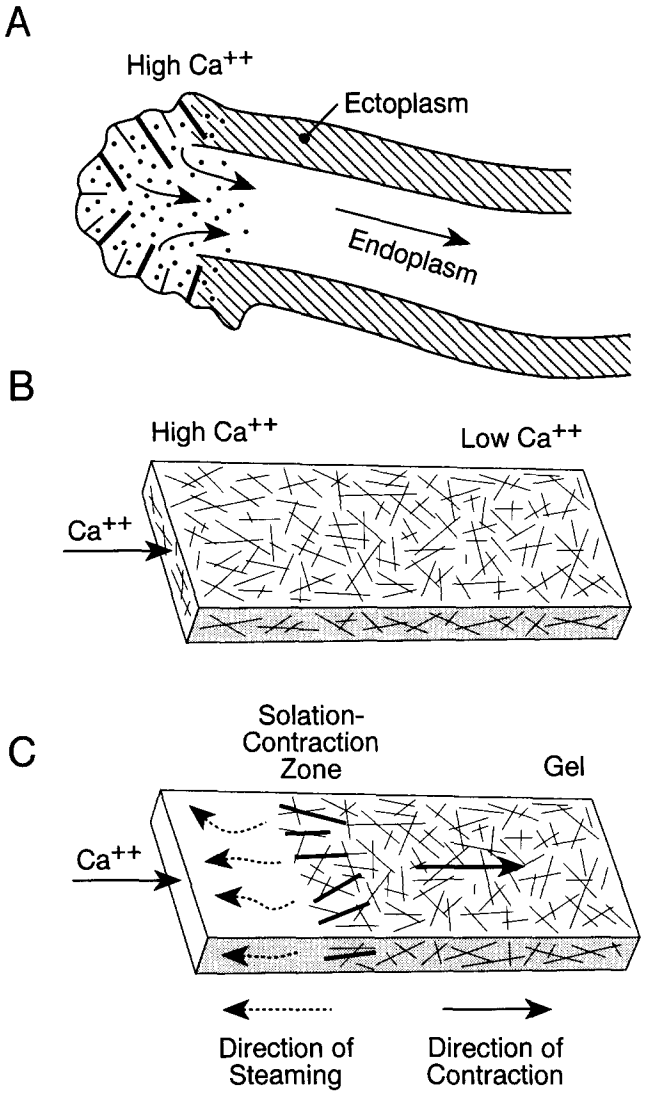

Figure 2. Correlation of the tail ectoplasm/endoplasm interface in amoeboid cells with the reconstituted models in microslides. (*A*) The zone of elevated free calcium in the tail ectoplasm exhibits both solation and contraction of the gelled ectoplasm to form endoplasm. The rate and extent of the two stages of solation is optimized to allow the forces of contraction to pull the tail forward toward the low calcium, maximally gelled ectoplasm, while permitting a self-destruction of the contracting ectoplasm to form endoplasm. (*B*) The reconstituted models form a gelled network that mimics the ectoplasmic tube. Addition of calcium at the proximal end of the microslide creates a gradient of free calcium, highest at the proximal end and lowest at the distal end. The low calcium distal end represents the more anterior ectoplasm in the amoeba and the high calcium proximal end represents the zone of high calcium in the tail ectoplasm. The ectoplasm-endoplasm interface is modeled at the proximal end where the calcium induces coupled solation and contraction. (*C*) Solation that includes the restriction of actin filament lengths can release some mass of the contracting gel as a sol. The contracting network forces the sol out of the gel under hydrostatic pressure. The direction of this streaming is in the direction of least resistance in the model, which is away from the contracting gel (see text).

The reconstituted samples in microslides were designed to mimic the ectoplasm in the rear of locomoting amoeboid cells (Fig. 2 *A*). The addition of Ca^{2+} to the proximal end of the model (Fig. 2 *B*) would initiate both solation of the gel and contraction due to the decreased resistance of the gel against actin-myosin II force generation. The assays were designed to identify sites of contraction, the direction of contraction relative to the low Ca^{2+} gelled region, sites of solation, and streaming activity (Fig. 2 *C*).

Proteins and Buffers

Column purified actin, gelsolin, Fx-45, myosin II, filamin, and the calcium-independent fragment of myosin light chain kinase (IMLCK) were purified, stored, and assayed as described in Janson et al. (1991) with the following changes. Immediately before use, column purified actin was clarified by centrifugation (100,000 *g*) and dialyzed against actin buffer (10 mM MOPS, pH 7.2, at 25°C, 10 mM EGTA, 0.2 mM ATP, 0.1 mM DTT, 0.005% Azide). Gelsolin and Fx-45 were dialyzed against gelsolin buffer (10 mM MOPS, pH 7.2, at 25°C, 100 mM $NaHCO_3$, 0.01 mM EGTA, 0.2 mM ATP, 0.1 mM DTT, 0.005% Azide). Myosin II was prepared for assays by suspension in myosin buffer (10 mM MOPS, pH 7.2, at 25°C, 50 mM $NaHCO_3$, 1 mM ATP, 1 mM $MgCl_2$, 0.1 mM DTT, 0.005% Azide) and clarification by centrifugation (30 s, 2,200 *g*). Immediately before use in the reconstituted system, phosphorylated myosin II was freshly diluted [1:3] with myosin dilution buffer (10 mM MOPS, pH 7.2, at 25°C, 50 mM $NaHCO_3$, 11 mM ATP, 15 mM $MgCl_2$, 0.1 mM DTT, 0.005% Azide). Before use in the reconstitution system, filamin was dialyzed against filamin buffer (10 mM MOPS, pH 7.2, at 25°C, 200 mM KCH_3COO, 0.1 mM DTT, 0.005% Azide). Calcium regulated *D. discoideum* α-actinin, purified by Dr. J. R. Simon according to Simon and Taylor (1986), was dialyzed against filamin buffer and assayed by falling ball viscometry with inclusion of either 1 mM $CaCl_2$ or 1 mM EGTA in the assay samples. The activity and contractions of the proteins were determined after final preparation and showed no significant changes from previously established activities with the buffer changes reported here (Janson et al., 1991).

The tetrasodium salt of Fluo-3 (Molecular Probes, Inc., Eugene, OR), a fluorescent calcium indicator, was suspended in filamin contraction buffer and added with the filamin to the reconstituted system at 10 μM final contraction. For addition of calcium to the reconstituted system (see below), 3.5 μl (10% of the final volume) of calcium buffer (0.1 mM $CaCl_2$, 10 mM MOPS, pH 7.2, at 25°C, 120 mM KCH_3COO, 10 mM $NaHCO_3$, 0.5 mM $MgCl_2$, 1.1 mM ATP, 0.11 mM EGTA, 0.1 mM DTT, 0.005% Azide) was gently added to one end (defined as the proximal end) of the sample using a Hamilton syringe. Control samples received 3.5 μl control buffer (calcium buffer with no calcium). Care was taken to not disturb the sample during application of the calcium or control solutions. The pH of all buffers was adjusted with ammonium hydroxide so additional ions would not affect final conditions. All buffers were degassed before use. For a complete review of preparation and testing of protein components and buffers see Janson (1991).

Preparation of Reconstituted Models

Reconstitution of the contractile system followed the same protocol as described in Janson et al. (1991) with changes noted below. Actin was polymerized with 100 mM KCH_3COO and 1 mM $MgCl_2$. 10.3 μm crimson, polystyrene latex beads (carboxylated) (Molecular Probes, Inc.) were included with the actin (100-fold dilution of stock beads). Inclusion of beads has previously been shown to have no effect on rates of contraction (Janson et al., 1991). Fx-45, which severs actin filaments in the absence of calcium, was added to initially produce actin filaments with an average length of 8–10 μm, defined by the technique of Janson et al. (1991), to insure a well-defined polymeric system. Calcium-regulated gelsolin or α-actinin, filamin, and freshly phosphorylated myosin II (phosphorylated with IMLCK under Ca^{2+}-free conditions) were added and gently vortexed. Samples were gently pipetted into 9 × 5 × 0.5 mm microslides (Vitro Dynamics, Rockaway, NJ), quickly placed under the microscope for observation, and maintained at 28°C using an air curtain with a temperature feedback circuit for the duration of the assay.

Gelsolin samples contained molar ratios of actin:gelsolin that would result in a calculated decrease in the length distribution to ca. 2 μm in the presence of elevated calcium (see Janson et al., 1991). α-actinin samples contained molar ratios of actin:α-actinin:filamin that, upon calcium addition, would reduce the relative cross-linking from ~1 cross-linking molecule (α-actinin and filamin) per 60 actin monomers to 1 cross-linking molecule (filamin alone) per 300 actin monomers (based on Flory theory, average filament length, and known α-actinin and filamin-binding stoichiometries). Thus, calcium would provide a fivefold decrease in gel structure due to cross-linking, although the minimum gel point (Flory, 1941; Hartwig and Stossel, 1979; Stossel, 1982) was maintained by filamin cross-linking even in the presence of calcium. Final protein concentrations and molar ratios for each sample system are shown (Fig. 3 *a*) and agree well with physiological values (Janson et al., 1991). Final buffer conditions closely match reported ionic conditions within mammalian nonmuscle cells (Fig. 3 *b*).

a)

Gelsolin Samples	α-actinin Samples
• 1.5 mg/ml actin with Fx-45 (10 μm actin filaments)	• 1.5 mg/ml actin with Fx-45 (10 μm actin filaments)
• Gelsolin to produce 2 μm actin filaments	• Calcium-regulated α-actinin (166:1 actin:α-actinin)
• Phosphorylated Myosin II (100:1 actin:myosin)	• Phosphorylated Myosin II (100:1 actin: myosin)
• Filamin (150:1 actin:filamin)	• Filamin (300:1 actin:filamin)

b)

Physiological Ion	Cellular Conditions	Reconstituted System
K^+	130-139 mM	120 mM
Na^+	12 - 20 mM	12.2 mM
Ca^{++}	0.01 - 5 mM	0 - 10 mM
Mg^{++}	0.1 - 1 mM	0.5 mM
Cl^-	1.5 - 4 mM	3.2 mM
HCO_3^-	12 mM	10.01 mM
pH	7.0 - 7.4	7.2

Figure 3. Summary of reconstituted system. (*a*) Protein concentrations and molar ratios (with respect to actin) for gelsolin samples and α-actinin samples. See Materials and Methods and Janson et al. (1991) for further details. (*b*) Final ionic conditions—Cellular vs Reconstituted System. Mammalian cellular conditions are taken from a general sample of the literature, summarized in Darnell et al. (1990).

Measurement of Calcium Rise and Contraction

For each sample, alternate images of Fluo-3 (Fluorescein filter set) and crimson bead (Texas-red filter set) fluorescence were acquired for 5 min without calcium at 30-s intervals. After addition of calcium buffer or control buffer (no calcium), images were acquired for 25 min using the same acquisition sequence and timing. Excitation light was blocked during interval times throughout acquisition to minimize the irradiance to the specimen. The samples were monitored using an Axioplan microscope (Carl Zeiss, Inc., Thornwood, NY) equipped with a 1.25 × Plan Neofluar objective, a 75 W XBO arc lamp, and an intensified C2400 CCD camera (Hamamatsu Photonics K.K., Hamamatsu City, Japan). Images were captured using a Macintosh-based, Technical Command Language package (BDS-Image, Biological Detection Systems, Inc., Pittsburgh, PA) and stored on a digital optical disk. Average velocities and the trajectories of crimson beads due to contraction were determined from stored images for equally defined proximal, middle, and distal areas of samples by manual tracking of movement of beads for each 30-s imaging interval. The movement of 100–300 beads from six Gelsolin samples and 30–70 beads from the three α-actinin samples were averaged for three periods—Pre-calcium, 0–5′ calcium, and 5–10′ calcium (see Figs. 4, 5, and 7). Average calcium concentration in identically defined proximal, middle, and distal areas was determined by measurement of average Fluo-3 fluorescence intensity of each area and direct comparison to a standard curve, generated using identically prepared samples with known calcium contractions. Streaming activity was also identified in the stored image data sets by direct analysis of crimson bead movement when contracting areas of the sample caused a flow of crimson beads. Analogous streaming movement is observed in motile amoebae and has been noted in previous in vitro studies using a gradient of cytochalasin D to induce solation of the gel (Janson et al., 1991).

Measurements of Calcium Rise and Solation

Reconstituted samples for determination of gel structure were identical to contraction samples except that myosin II was unphosphorylated and 0.264 μm polystyrene latex beads were included which had been coated with 2% BSA to inhibit any bead/protein interactions (Hou et al., 1990). Because myosin was unphosphorylated, no active contractions could occur in the reconstituted samples. Diffusion of the beads was imaged and recorded on video tape using Video-enhanced interference contrast microscopy with an Axiophot microscope, 100×, 1.3 NA, Neofluar objective, 1.4 NA condenser, a 2 × optivar (Carl Zeiss, Inc.), a C-2400 camera, and an Argus-10 image processor (Hamamatsu Photonics). Movement of seven to thirty beads in proximal, middle, and distal areas of each sample was determined for each 30-s period over the 5-min intervals corresponding to times reported for contraction data. The diffusion coefficient, D, of the 0.264 μm beads was calculated from these measurements, using the random walk equation $D = (\partial x)^2/4t$ (Hou et al., 1990) (see Figs. 5 and 7).

Electron Microscopy

Samples prepared in an identical manner to contraction samples above, were processed and imaged by electron microscopy using the method of Ris (1985) with minor adaptations to better preserve and image network components. See Janson (1991) for a detailed description of preparation of samples for EM.

Results

The use of multi-mode microscopy and a reconstituted system capable of calcium-activated, physiological solation allowed the measurement of contraction and streaming (assayed by measuring velocities of crimson beads), calcium levels (assayed by Fluo-3 fluorescence), and solation of parallel samples (assayed by measuring the diffusion of polystyrene latex beads). The measurement of these parameters in three separate areas of progressively solating samples allowed a direct measure of the effect of decreasing gel structure on the rate of contraction and ability to cause streaming in a model system that mimics the proteins and dynamics of many amoeboid cells. The shortening of actin filaments by gelsolin and decreased cross-linking of actin filaments by inhibition of α-actinin cross-linking were used as two independent methods of solating the gel. The proximal region of the model is the site of calcium addition and models the tail ectoplasm of locomoting amoeboid cells, less the posterior membrane (Fig. 2, *A* and *B*). This is also where the highest free calcium concentration is found (Taylor et al., 1980 *a*,*b*; Brundage et al., 1991). The middle and distal regions of the model represent more anterior regions of the ectoplasm (gelled cell cortex) that are at lower free calcium ion concentrations (see Fig. 5).

Gelsolin Samples Exhibit Cytoplasmic Streaming as well as a Self-Destruct, Solation-Contraction

Preceding calcium addition, the average velocity of crimson beads in gelsolin samples was ~0 μm/s (no contraction) in the proximal, middle, and distal areas of the sample (Figs. 4 *a* and 5 *a*) since gel strength resisted the forces of the myosin motors. Measurement of bead diffusion (*D*) in the parallel sample indicated a gelated sample in all three areas (Fig. 5 *a*). Examination of samples without added calcium, by electron microscopy, also indicated a high degree of network structure (Fig. 6 *a*; see also Hartwig and Stossel, 1979, for

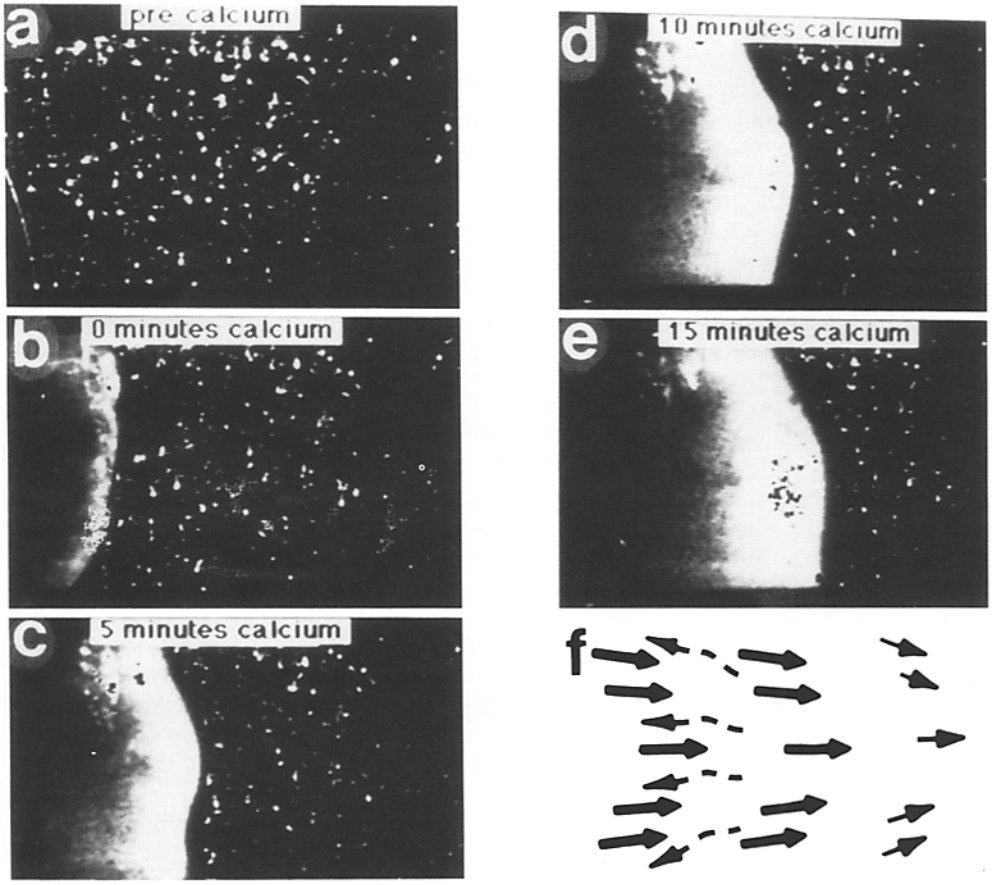

Figure 4. Sequence of calcium-induced contraction of a gelsolin sample. (*a*) *pre* Ca^{2+}, crimson bead fluorescence before addition of calcium. (*b*) *0 min*, calcium (seen as *thin, bright white area*) added to proximal end (*left side of picture*) of capillary. (*c*, *d*, and *e*) Progression of calcium gradient (*bright white areas*) and crimson bead movement induced by contraction at (*c*) t = 5 min, (*d*) t = 10 min, and (*e*) t = 15 min. Calcium fluorescence image and crimson bead fluorescence image (acquired separately during experiments) are overlaid in this figure using NIH Image (National Institute of Mental Health, Research Services Branch) to show relative positions of calcium gradient and gel sample (*beads*). (*f*) Summary of contraction for 0–15 min. Solid arrows illustrate overall movement of beads showing average speed and direction during assay time. Dashed arrows depict direction of streaming.

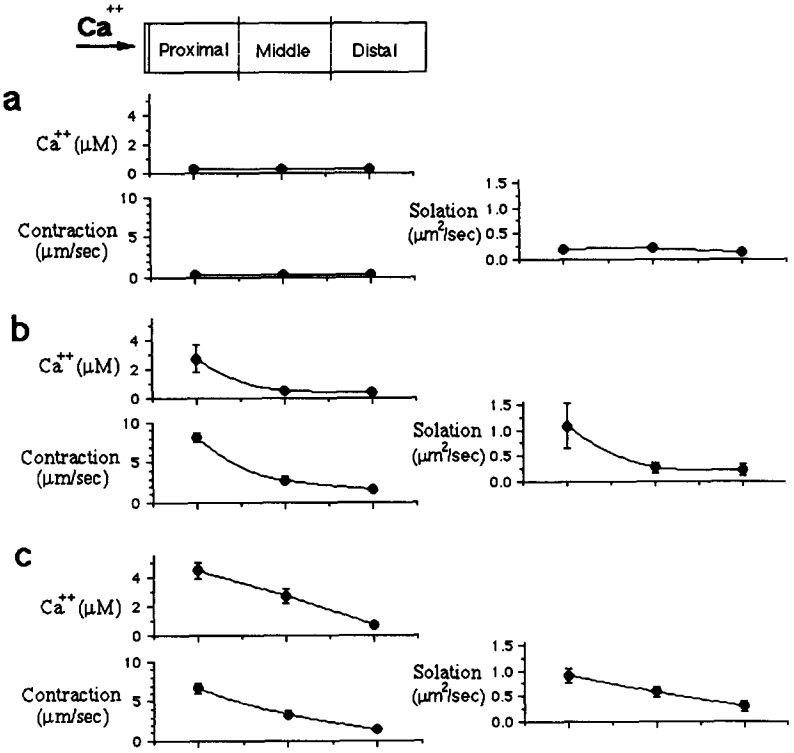

Figure 5. Solation-contraction of gelsolin samples with fully phosphorylated myosin II. Calcium concentration (μM), average velocity of crimson beads during contraction ($\mu m/s$) of crimson beads, and solation of polystyrene latex beads, measured in parallel samples by determining the diffusion coefficient D ($\mu m^2/s$), in proximal, middle, and distal areas at (*a*) pre-Calcium, (*b*) 0–5 min after calcium addition, and (*c*) 5–10 min after calcium addition times. Calcium was added at left (*proximal*) end of the respective chamber (see *a*). Error bars represent ±1 SD.

representative micrographs). Calcium added at one end of the microslide chambers activated gelsolin molecules within the sample and initiated solation (partial solation) in the proximal area while only minimally solating the middle area and did not affect the gel structure of the distal area over the ten minute assay time (see Figs. 4 and 5). During the period 0–5 min immediately after addition of the calcium gradient, directed crimson bead velocity in the proximal area, reflecting the contraction, increased dramatically (8.19 μm/s) while beads in the middle and distal areas showed only slight movements (Figs. 4 *b* and *c* and 5 *b*). During the period 5–10 min after application of calcium, the proximal beads maintained their velocity, while the velocity of the middle area beads continued to increase as calcium levels rose and this region began to solate and contract (Figs. 4 *c* and *d* and 5 *c*). After 10 min, the proximal area had completely contracted into the middle area while the middle area continued to contract faster than the distal area (Fig. 5 *c*). The direction of contraction was always toward the more gelled regions which functioned as an anchor for the contractile forces, mimicking the retraction of tails in amoeboid cells. Control samples with only final reconstitution buffer (no calcium) added, displayed only very slow, random contractions. The very slow contractions in the controls were probably due to the ability of the fully phosphorylated myosin II to slowly overcome the load imposed by the gel structure (Giuliano et al., 1992).

Components of the solating and contracting gel were driven out of the contracting gel and exhibited streaming as noted by the flow of crimson beads (see Fig. 4 *f*). This streaming activity was comparable to earlier results using cytochalasin D as an initiator of solation and contraction (Janson et al., 1991). Like cytochalasin D, gelsolin shortens actin filaments. Gelsolin activity solated the gel below the gel point, allowing subunits to be forced out of the gel during contraction. Electron micrographs of gelsolin samples where contraction was initiated with calcium, demonstrated the formation of dense fibers (Fig. 6 *B*), as well as the presence of short actin filaments which appeared to have been expelled from the contracting network (Fig. 6 *E*). Control samples showed no streaming by crimson bead movement and no expulsion of filaments by electron microscopy. Samples with an excess of gelsolin (≥10-fold higher), producing very short actin filaments (< 0.2 μm), did not contract since this condition would lower the gel state below the calculated gel point necessary for transmitting tension (Taylor and Fechheimer, 1982; Janson et al., 1991) (see Fig. 1 *c*).

α-Actinin Samples Show Solation-Contraction with No Streaming

Calcium gradients in samples with both α-actinin and filamin cross-linkers, containing fully phosphorylated myosin II, were essentially identical to gelsolin samples (see Fig. 4), although movement of the calcium gradient through the sample was slower (compare Figs. 5 *b* and 7 *b*), possibly due to the absence of flow induced by cytoplasmic streaming and a slower wave of contraction through the sample (see also Discussion). Before addition of calcium, the velocity of crimson beads in the proximal, middle, and distal areas of the microslide chambers was 0 μm/s (Fig. 7 *a*). After the initiation of a calcium gradient, crimson bead velocity rose in the proximal area of samples (2.25 μm/s) in response to the increased calcium level, while moderate increases were

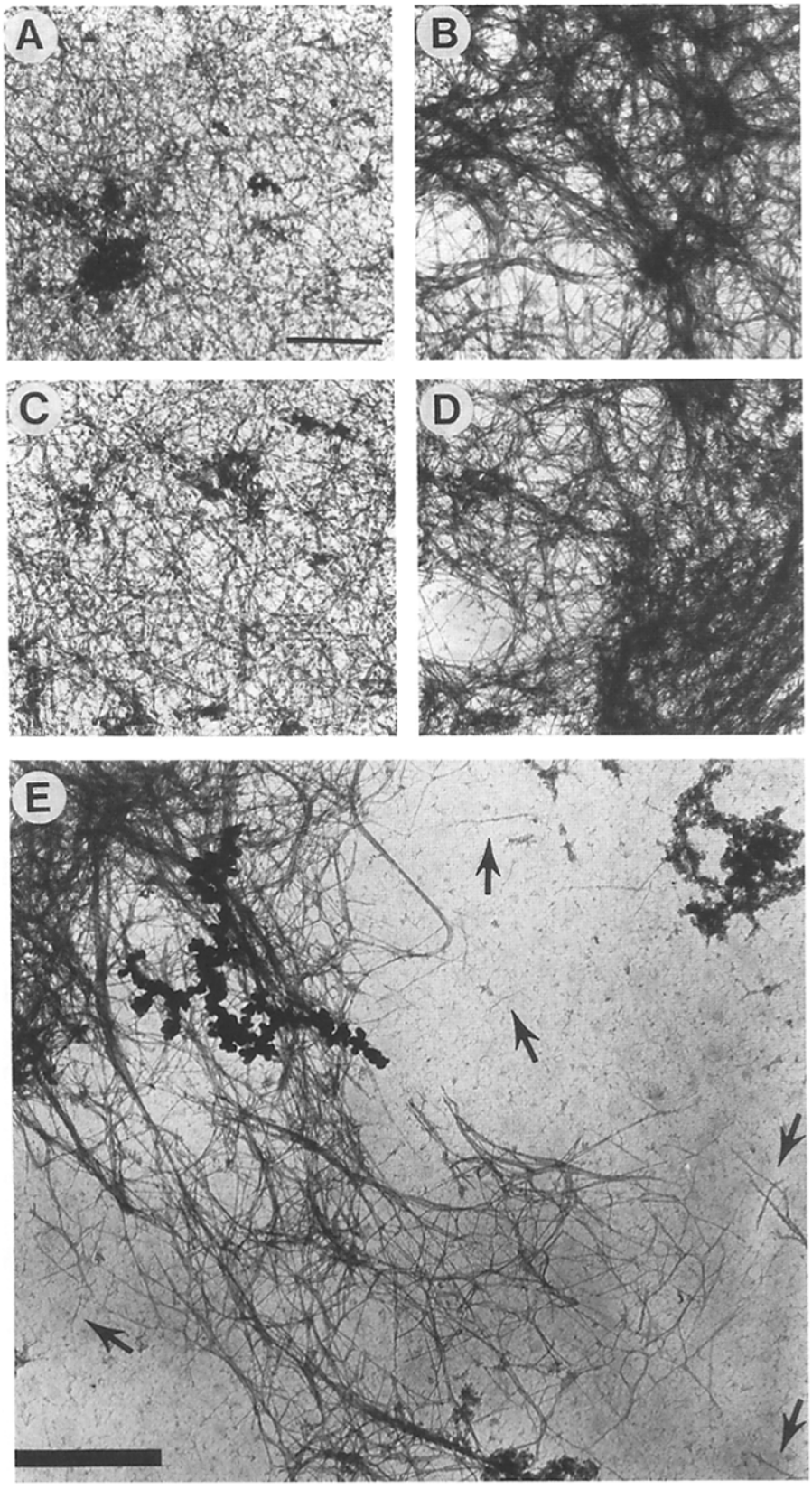

Figure 6. Structure of reconstituted samples ± calcium by electron microscopy. Samples prepared and imaged as described in the text. (*A*) Gelsolin sample without addition of calcium shows isotropic gel network. (*B*) Gelsolin sample with calcium displays domains of concentration and alignment of actin filaments. (*C*) α-actinin sample without calcium also shows isotropic gel network. (*D*) α-actinin sample with calcium also displays domains of concentration and alignment of actin. Bar, 1 μm. (*E*) Loss/expulsion of solated material from contracting gelsolin samples. Electron micrograph shows edge of contracting sample and small actin filaments (*arrows*). These filaments were always seen in contracting gelsolin samples with added calcium. This material was not seen in gelsolin samples without calcium, α-actinin samples with or without calcium, or actin samples alone. See text for further details and discussion. Bar, 0.5 μm.

noted in the middle area and no increase was measured in the distal area vs control values (Fig. 7 *b*). During 5–10 and 10–15 min post-calcium addition periods, proximal area crimson bead velocities remained high (although lower than gelsolin samples, Fig. 5), while middle and distal bead velocities continued to rise as calcium levels increased (Fig. 7 *c*). Electron microscopy also indicated contraction in α-actinin samples by the formation of dense arrays of actin

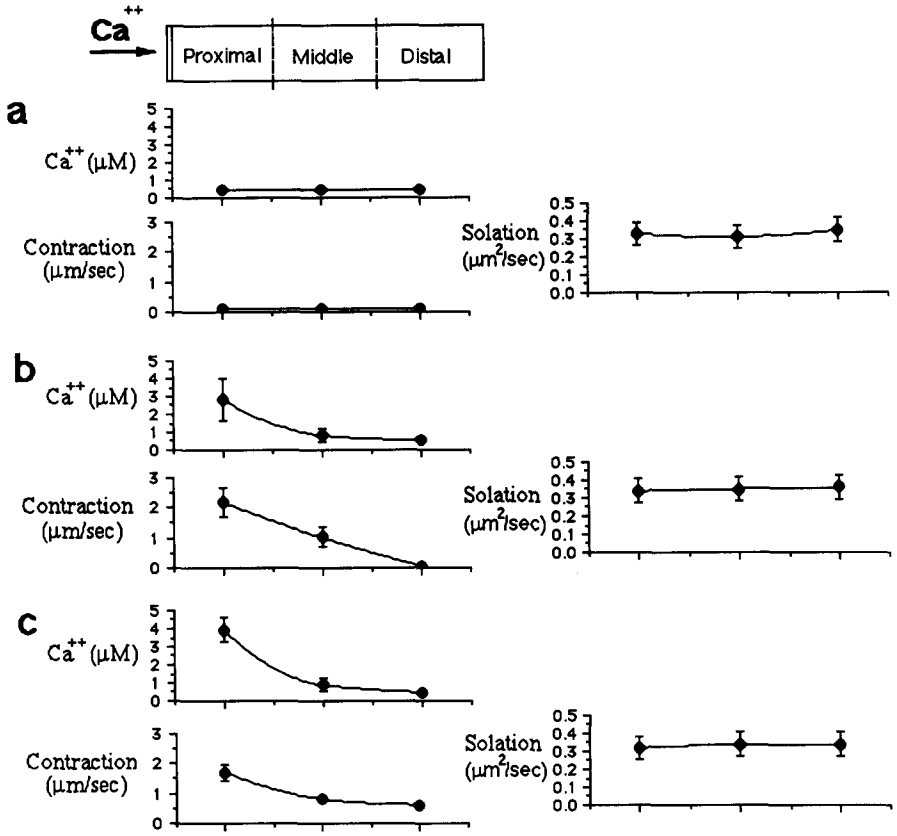

Figure 7. Solation-contraction of α-actinin samples with fully phosphorylated myosin II. Calcium concentration (*μM*), average velocity of crimson beads during contraction (*μm/s*) of crimson beads, and solation of polystyrene latex beads, measured in parallel samples by determining the diffusion coefficient D ($\mu m^2/s$), in proximal, middle, and distal areas at (*a*) pre-Calcium, (*b*) 0–5 min after calcium addition, and (*c*) 5–10 min after calcium addition times. Calcium was added at left (*proximal*) end of the respective chamber (see *a*). Error bars represent ±1 SD.

from the uncontracted, isotropic gel (Fig. 6, *C* and *D*). Control samples without calcium displayed slow contractions (0.24 μm/s average velocity for all areas over 15 min) without streaming.

The lower rate of contraction in the α-actinin samples compared to the gelsolin sample probably reflects the higher load placed on the myosin II motors by the actin filaments, filamin, and, before calcium addition, the α-actinin cross-linking activity. Additionally, since no gel material was released during the contraction (see below), as the contraction progressed the microscopic concentration of actin filaments and filamin would continually rise as the gel became smaller but all gel material remained. This relative increase in actin and filamin cross-linkers would provide an ever-increasing load on the myosin motors by filament entanglement and cross-links, slowing contraction.

The solation bead assay in the parallel sample did not indicate a measurable solation in any of the three areas, despite adequate calcium levels. This absence of increased bead diffusion in the α-actinin samples may be due to the high on/off rate of α-actinin. Since a single α-actinin molecule maintains the gel structure for only 0.5–0.005 s (Sato et al., 1987), bead movement may only be affected by the longer-lived filamin cross-linking (≥ 100 s) which is unaffected by calcium (Janmey et al., 1990). Filamin concentrations used in the α-actinin samples were only high enough to provide slightly higher than the minimal gel structure required to maintain an infinite network based on actin filament lengths and known filamin-binding parameters (Flory, 1941; Hartwig and Stossel, 1979; Janmey et al., 1990; Janson et al., 1991). This low level of filamin gel structure would allow high rates of bead diffusion in the α-actinin samples with or without calcium (see Fig. 7, *a–c*). Thus, despite microscopic inhibition of α-actinin cross-linking, calcium-dependent solation and increased macroscopic movement of the beads would be masked as has been seen in other studies (Sato et al., 1987; Simon et al., 1988). Although macroscopic movements of beads would not be changed, the microscopic decrease in the relative cross-linking number as calcium diffused into the gel and inhibited α-actinin cross-linking would allow the myosin tension to overcome the reduced counterforces of the gel structure, resulting in contraction.

No streaming activity was detected in α-actinin samples since no gelsolin was present to take apart the contracting gel. Additionally, no short actin filaments were generated during the contraction as determined by electron microscopy.

Discussion

The wide range of phenotypes of amoeboid movement, ranging from pseudopod extension, cytoplasmic streaming, and tail retraction in free-living amoebae, leukocytes, macrophages, and slime molds, to the slow extension and retraction of lammellipodia and retraction of tails in fibroblasts could be due to distinct mechanisms. Alternatively, the same mechanisms may simply be expressed at a different rate and to a different extent in various amoeboid cells (Taylor and Condeelis, 1979). Our basic assumption is that there are multiple forces that are integrated to yield normal amoeboid

movements, including mechanisms responsible for the initiation and extension of pseudopods, the transport of cytoskeletal subunits to the leading edge of extending cells, and the retraction of tails. Myosin I motors could be locally involved in movements at the leading edge of amoeboid cells, since it is identified at the tips of extending pseudopods while myosin II is absent (Fukui et al., 1989; Conrad et al., 1993). Myosin II, which is more highly concentrated in posterior regions of migrating cells, could be predominantly involved in tail contraction and related streaming activity. This discussion will focus on the possible relationship between gel-sol transitions and contraction caused by myosin II in these regions.

Role of Actin-binding Proteins in Gel-Sol Changes

The actin-binding cytoskeleton of amoeboid cells, including actin filaments and actin-binding proteins, plays a key role in the determination of cell shape and motility. Among the large array of actin-binding proteins are actin filament severing proteins (e.g., gelsolin), which regulate length distribution and actin cross-linking proteins (e.g., filamin, α-actinin) which form interfilament cross-links (Taylor and Condeelis, 1979; Stossel et al., 1985; Pollard and Cooper, 1986). The activities of these actin severing and actin cross-linking proteins are often regulated by ionic changes such as pH, pCa^{2+}, binding of lipid metabolites, and posttranslational modifications such as phosphorylation. Changing the activities of these proteins with these regulatory second messengers may substantially change the gel structure of the cytoskeleton (Hellewell and Taylor, 1979; Hartwig and Stossel, 1979; Luby-Phelps et al., 1988; Janmey et al., 1990). A two stage solation process based on increased actin filament severing activity and/or a decrease in the relative number of cross-links per length of actin filament can lead to a decrease in the strength of the gel (partial solation) to the complete loss of gel structure when the network is decreased below the gel point (complete solation). Alternatively, inhibition of severing activity and/or an increase in the relative cross-linking number leads to increased gelation and gel strength.

Solation-Contraction Coupling Hypothesis Explains the Dynamics of the Reconstituted Models

The solation-contraction hypothesis has evolved based on studies on single cell models (Taylor et al., 1973), cytoplasmic extracts (Condeelis and Taylor, 1977; Hellewell and Taylor, 1979; Taylor and Fechheimer, 1982), reconstituted models (Janson et al., 1991) as well as fixed (Conrad et al., 1993) and living cells (Taylor et al., 1980 *a,b*; Kolega et al., 1991). This hypothesis contains six major proposals describing how changing the gel state of the actin-based cytoskeleton may play a significant role in regulating the actin/myosin II contraction (Taylor and Fechheimer, 1982; Kolega et al., 1991; Janson et al., 1991). These six proposals include (1) the actin filament-based cytoskeleton is a significant structural component of the cytoplasm composed of a network of actin filaments and actin-binding proteins. The gel strength can be at one of three levels: (*a*) an infinite network, but with the minimal number of cross-links to attain the gel point; (*b*) a gel with greater than the minimal number of cross-links to reach the gel point; and (*c*) a sol that cannot transmit tension over domains greater than the remaining cross-linked network. The gel may be made weaker or stronger dependent on actin filament length and the relative cross-linking number; (2) a gel resists contractions by offering counterforces to the myosin motors (a load on the motors). In a highly gelled system, no contraction will occur despite the presence of active, cycling myosin molecules; (3) the gel strength may be decreased through dissociation of cross-links between filaments and/or by restrictions of actin filament lengths while still maintaining the infinite network (partial solation); (4) a minimum level of gel structure (the gel point) is required to transmit the contraction forces through the connected network; below the gel point (complete solation), only unproductive actin-myosin interactions occur; (5) cytoplasmic contractions can be induced when the weakened gel is unable to resist the force of the myosin molecules. Usually, an increase in the activation of the motors parallels weakening of the gel; (6) continued breakdown of the gel, involving factors that restrict the length of actin filaments, releases solated gel subunits into the soluble cytoplasm. This completes solation-contraction coupling which is a self-destruct process. The released subunits are then available for diffusion or transport to sites of assembly and gelation.

In the present model system, a partial solation caused by a gradient of free calcium ion concentration allowed direct comparison of contraction in both solating and gelled areas of the models. The solating areas differed from gelled regions in the gelsolin samples by a decrease in average actin filament length from 10 to a minimum of 2 μm (see Materials and Methods and Janson et al., 1991). Samples containing α-actinin, but no gelsolin, allowed tests of how reversible cross-linking may regulate contraction without a self-destruct process of shortening actin filaments. In all cases, decreasing the counterforces to contraction of a gel network (partial solation), either by activation of gelsolin or inhibition of α-actinin cross-linking, led to a marked increase in the velocity of contraction (Figs. 4, 5, and 7). Highly gelled samples showed little or no signs of contraction until solation was initiated, even though myosin II was fully phosphorylated, filamentous, and active. Therefore, fully active myosin II could not overcome the counterforces of a maximally gelled system. However, weakening the counterforces in the gel either by restricting the length of actin filaments (gelsolin sample) or by decreasing the number of cross-linkers (α-actinin sample) permitted myosin II to perform work on the remaining network.

Examination of contracting networks by electron microscopy confirmed these results (Fig. 6, *A–D*). Electron microscopy indicated the production and expulsion of very short actin filaments in samples containing activated gelsolin (Fig. 6 *E*; see also Stossel, 1982; Stossel et al., 1985), which may reflect the gel components that stream out of the contracting gel. Therefore, the "self-destruct" contraction that occurs when molecules such as gelsolin decrease the gel structure of the contracting network can also produce the material that can be driven out of the contracting network by positive hydrostatic pressure (Fig. 8). This self-destruct contractile process requires control of the rate and extent of solation relative to contraction. It has been demonstrated (Stendahl and Stossel, 1980; Janson et al., 1991; this study) that too rapid and extensive a solation of the gel can actually inhibit the contraction. Electron microscopy of α-actinin samples

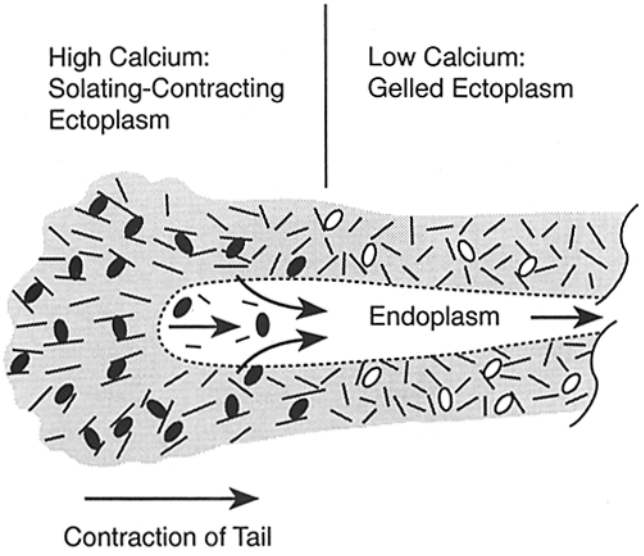

Figure 8. Solation-contraction coupling and tail retraction. Diagram depicts the cortical gel layer in the tail of an amoeboid cell exhibiting cytoplasmic streaming and tail retraction. The cortical gel is represented by the short filaments and myosin II motors are represented by open ellipses (*minimally activated*) and filled ellipses (*maximally activated*). No actin cross-linking proteins are shown to simplify the diagram. Regions of high and low free calcium ion concentration are also indicated. The elevation of free calcium in the tail cortex decreases the counterforces of the gel (*partial solation*) by restricting the lengths of actin filaments and by dissociating some actin binding proteins. The myosin motors also become maximally activated through a calcium regulated phosphorylation of myosin II. The transformation of the maximally gelled cortex into a partially solated-contracting gel generates a positive hydrostatic pressure against the completely solated fraction which is the newly formed endoplasm. The rate and extent of solation are balanced against the forces applied to the weakened gel by the myosin II motors. During contraction, the myosin motors order some of the actin filaments and align domains of the weakened gel in the tail ectoplasm (see Taylor et al., 1973; Taylor et al., 1980*a*, *b*). The contracting tail is pulled forward toward the low calcium, higher gel strength ectoplasm anterior to the tail. The retraction of the contracting tail towards the more gelled ectoplasm anterior to the tail optimizes cell polarity since no new protrusion can form against the contracting gel attached to the membrane. As the contraction continues, complete solation occurs and generates the endoplasm. Cortical flow of the actin-based gel from the anterior of the cell to the posterior propagates the cycle of ectoplasm to endoplasm. Furthermore, the contraction of the tail cortex actually drives the solating domains forward as part of the endoplasm by positive hydrostatic pressure.

showed no release of material, indicating that the gel remained intact throughout the contraction process. Additionally, no streaming activity was noted in any of the α-actinin samples since the absence of gelsolin resulted in no released mass of the gel. As noted above, contraction without release of gel material may offer additional control of contraction rate, especially as the contraction progresses and localized concentrations of actin and actin-binding proteins increase.

Therefore, the gel strength of the actin cytoskeleton can regulate the work performed by myosin motors by either limiting the actin-myosin interactions to an isometric contraction (high gel strength) or initiating isotonic contractions (partial solation). Measurement of the gel state by measuring the diffusion of beads directly defined the gradient of solation, highest at the high calcium, proximal end and lowest at the low calcium, distal end of the models (Fig. 5). Since the proximal end contracted fastest in all samples, followed by the middle area, solation must also promote contraction. If increased gel strength promoted contraction, the middle and distal ends of the model would necessarily contract faster than the proximal end (Janson et al., 1991). All results show that decreasing gel strength may both initiate and accelerate actin/myosin II contractions (Figs. 4, 5, and 7) as long as there is a threshold amount of network structure to transmit tension. It is important to note that in a contracting gel, myosin II motors serve as both the motor force and cross-linkers to maintain part of the network structure required to transmit the tension.

Solation-Contraction Coupling Plays a Role in Amoeboid Movement

The mechanism of movement of an amoeboid cell is probably dependent on several integrated mechanisms, including actin assembly-disassembly, sol-gel changes, osmotic pressure gradients, and myosin motor activities. Solation-contraction coupling of an actin/myosin II-based cortical gel can explain tail retraction, transformation of ectoplasm into endoplasm, and transport of cytoplasm out of tails of amoeboid cells. Solation of the gel is initiated in the high Ca^{2+} tail region, which permits an isotonic contraction along with the calcium-induced phosphorylation and concomitant activation of myosin II. The coupling of the partial solation and contraction in the tail ectoplasm is predicted to generate forces for tail retraction, while ultimately producing the sol that forms the endoplasm in the tail (Taylor, 1977). This relationship also insures that a contracted mass of cytoplasm does not accumulate in the tail, but rather a smooth transition between ectoplasm and endoplasm occurs. The coupling of solation and contraction in the tail is also a mechanism by which the actin-based cytoskeleton can be recycled to the leading edge (Conrad et al., 1993; Gough and Taylor, 1993), a necessary step in cortical flow (Bray and White, 1988). In addition, the self-destruct contraction of the tail ectoplasm would be predicted to generate a positive hydrostatic pressure on the maximally solated fraction of the ectoplasm (endoplasm) which is driven forward as the streaming endoplasm (Taylor and Fechheimer, 1982). The streaming endoplasm returns subunits to the leading edge (up to 1 mm away from the tail in some free-living amoebae) where gelation occurs to form the ectoplasmic tube.

The direction of contraction of the in vitro model is consistent with the direction of contraction of the tail ectoplasm in vivo since the contraction works against the distal gel (Fig. 2, *A* and *B*). We note, however, the direction of streaming in the model is in the opposite direction to that observed in the tail of the amoeba (Fig. 2, *A* and *C*). The maximally solating and contracting gel model would force both syneretic fluid and solated fractions out of the network under positive hydrostatic pressure. In the absence of a closed, membrane-bound tube of ectoplasm and central core of endoplasm, as found in the living cell, this streaming activity would follow the route of least resistance in the in vitro model, which is away from the contracting gel (Fig. 2 *C*).

In a living cell, however, the contracting tail ectoplasm would work against the more rigid, gelled anterior ectoplasm and would be pulled forward resulting in tail retraction (Fig. 8). The central core of endoplasm, inside the ectoplasmic tube, would also provide a low-resistance area for forward streaming of the solated gel (endoplasm). Attachment of the tail to the substrate would function as an additional load for the contracting tail (Chen, 1981).

The solation-contraction coupling hypothesis can explain the dynamics of the model system described here, the conversion from cortical ectoplasm to endoplasm, the retraction of tails, and the production of a positive hydrostatic pressure that could produce some of the force required for cytoplasmic transport into pseudopods (cytoplasmic streaming in some amoeboid cells). Solation-contraction coupling may also play an important role in other mechanisms involved in amoeboid movement as well as other motility processes.

Amoeboid movement also involves the extension of pseudopods which may involve osmotic pressure, the regulation of actin assembly, the activity of other myosin motors (Conrad et al., 1993), and sol-gel transformations at the tips of the advancing pseudopods (Oster and Perelson, 1987). Regulatory events in pseudopods may, therefore, be directly related to dynamic events in the tails and in the endoplasm. At the minimum, there must be some form of coordination between the formation of extending pseudopods, the transport of cytoplasm, and the retraction of tails in order to yield continuous movements (Trinkaus, 1980; Taylor et al., 1980 *a*,*b*; Chen, 1981).

We also suggest that other contractile events, such as cytokinesis, involve solation-contraction coupling since a self-destruct contraction process is predicted to explain the absence of a dense contracted mass between daughter cells at the completion of division. In contrast, contractile processes that do not involve breakdown of the gel network (e.g., α-actinin samples) could effectively slow and stop the contraction, resulting in a dense mass. However, the activation of actin-severing proteins could effectively convert such a contraction to a self-destruct process allowing the release of gel components and continued contraction.

The solation-contraction coupling hypothesis, integrated with the concepts expressed as cortical flow by Bray and White (1988), could form one of the central tenets of normal cell movements, including amoeboid movements and cytokinesis, and provides a unified and important framework for continued study of these and other contractile events.

The authors gratefully acknowledge the stimulating discussions with Dr. Fred Lanni, Dr. Kevin Burton, Dr. Ken Giuliano, and Dr. John Kolega. We also acknowledge the critical enthusiasm of one of our reviewers who encouraged us to improve the description of the hypothesis. The authors would also like to thank Dr. Gregory Fisher and Mr. Joe Suhan for help with electron microscopy.

This work was supported by National Institutes of Health (NIH) grant AR-32461 and National Science Foundation Science and Technology Center grant DIR-81920118 to D. L. Taylor and an NIH Predoctoral Training grant 5T32GM08067 to L. W. Janson. L. W. Janson is currently a National Research Council Postdoctoral Fellow at NASA–Johnson Space Center, Houston, TX.

Received for publication 7 January 1993 and in revised form 2 July 1993.

References

Abercrombie, M. 1980. The crawling movement of metazoan cells. *Proc. R. Soc. Lond. B. Biol. Sci.* 207:129–147.

Allen, R. D. 1973. Biophysical aspects of pseudopodium formation and retraction. *In* The Biology of Amoeba. K. W. Jeon, editor. Academic Press, New York. 201–247.

Bray, D., and J. White. 1988. Cortical flow in animal cells. *Science (Wash. DC).* 239:883–888.

Brundage, R., K. Fogarty, R. Tuft, and F. Fay. 1991. Calcium gradients underlying polarization and chemotaxis of eosinophils. *Science (Wash. DC).* 254:703–706.

Chen, W.-T. 1981. Mechanism of retraction of the trailing edge during fibroblast movement. *J. Cell Biol.* 90:187–200.

Condeelis, J. 1992. Are all pseudopods created equal? *Cell Motil. Cytoskeleton.* 22:1–6.

Condeelis, J. S., and D. L. Taylor. 1977. The contractile basis of amoeboid movement. V. The control of gelation, solation, and contraction in extracts from Dictyostelium discoideum. *J. Cell Biol.* 74:901–927.

Conrad, P. A., K. Giuliano, G. Fisher, K. Collins, P. Matsudaira, and D. L. Taylor. 1993. Relative distribution of actin, myosin I, and myosin II during the wound healing response of fibroblasts. *J. Cell Biol.* 120:1381–1391.

Darnell, J., H. Lodish, and D. Baltimore. 1990. Molecular Biology of the Cell. Scientific American Books, Inc., New York. 136 pp.

DeBiasio, R. L., L.-L. Wang, G. W. Fisher, and D. L. Taylor. 1988. The dynamic distribution of fluorescent analogues of actin and myosin in protrusions at the leading edge of migrating Swiss 3T3 fibroblasts. *J. Cell Biol.* 107:2631–2645.

DeLozanne, A., and J. Spudich. 1987. Disruption of the Dictyostelium myosin heavy chain gene by homologous recombination. *Science (Wash. DC).* 236:1086–1091.

Fisher, G. W., P. Conrad, R. L. DeBiasio, and D. L. Taylor. 1988. Centripetal transport of cytoplasm, actin, and the cell surface in lamellipodia of fibroblasts. *Cell Motil. Cytoskeleton.* 11:235–247.

Flory, P. J. 1941. Molecular size distribution in three dimensional polymers. I. Gelation. *J. Amer. Chem. Soc.* 63:3083–3090.

Fukui, Y, T. J. Lynch, H. Brzeska, and E. D. Korn. 1989. Myosin I is located at the leading edges of locomoting Dictyostelium amoeba. *Nature (Lond.).* 341:328–331.

Giuliano, K., J. Kolega, R. DeBiasio, and D. L. Taylor. 1992. Myosin II phosphorylation and the dynamics of stress fibers in serum-deprived and stimulated fibroblasts. *Mol. Biol. Cell.* 3:1037–1048.

Gough, A. H., and D. L. Taylor. 1993. Fluorescence anisotropy imaging microscopy maps calmodulin binding during cellular contraction and locomotion. *J. Cell Biol.* In press.

Grebecki, L. 1982. Local contraction and the new front formation site in Amoeba proteus. *Protistologica.* 28:397–402.

Hahn, K., R. DeBiasio, and D. L. Taylor. 1992. Patterns of elevated free calcium and calmodulin activation in living cells. *Nature (Lond.)* 359:736–738.

Hartwig, J. H., and T. P. Stossel. 1979. Cytochalasin B and the structure of actin gels. *J. Mol. Biol.* 134:539–553.

Hellewell, S. B., and D. L. Taylor. 1979. The contractile basis of amoeboid movement. VI. The solation-contraction coupling hypothesis. *J. Cell Biol.* 83:633–648.

Honer, B., S. Citi, J. Kendrick-Jones, and B. M. Jochrush. 1988. Modulation of cellular morphology and locomotary activity by antibodies against myosin. *J. Cell Biol.* 107:2181–2189.

Hou, L., K. Luby-Phelps, and F. Lanni. 1990. Brownian motion of inert tracer macromolecules in polymerized and spontaneously bundled mixtures of actin and filamin. *J. Cell Biol.* 110:1645–1654.

Janson, L. W. 1991. Regulation of actin/myosin II-based contraction in nonmuscle cells by solation-contraction coupling. Ph.D. thesis. Carnegie Mellon University, Pittsburgh, Pennsylvania.

Janson, L.W., J. Kolega, and D. L. Taylor. 1991. Modulation of contraction by gelsolin/solation in a reconstituted motile model. *J. Cell Biol.* 114: 1005–1015.

Janson, L. W., J. R. Sellers, and D. L. Taylor. 1992. Actin-binding proteins regulate the work performed by myosin II motors on single actin filaments. *Cell Motil. Cytoskeleton.* 22:274–280.

Janmey, P. A., S. Hvidt, J. Lamb, and T. P. Stossel. 1990. Resemblance of actin-binding protein/actin gels to covalently crosslinked networks. *Nature (Lond.).* 345:89–92.

Knecht, D., and W. Loomis. 1987. Anti-sense RNA inactivation of myosin heavy chain gene expression in D. discoideum. *Science (Wash. DC).* 236: 1081–1086.

Kolega, J., L. W. Janson, and D. L. Taylor. 1991. The role of solation-contraction coupling in regulating stress fiber dynamics in non-muscle cells. *J. Cell Biol.* 114:993–1003.

Komnick, H., W. Stockem, and K. E. Wohlfarth-Bottermann. 1973. Cell motility: mechanisms in protoplasmic streaming and amoeboid movement. *Int. Rev. Cytol.* 34:169–249.

Luby-Phelps, K., F. Lanni, and D. L. Taylor. 1988. The submicroscopic properties of cytoplasm as a determinant of cellular function. *Annu. Rev. Biophys. Biophys. Chem.* 17:369–396.

Oster, G. F., and A. S. Perelson. 1987. The physics of cell motility. *J. Cell Sci.* 8 (Suppl.):35–54.

Pantin, C. F. A. 1923. On the physiology of amoeboid movement. *J. Mar. Biol. Assoc. U. K.* 13:24.

Pollard, T. D., and J. A. Cooper. 1986. Actin and actin-binding proteins. A

critical evaluation of mechanism and function. *Annu. Rev. Biochem.* 55: 987–1035.

Ris, H. 1985. The cytoplasmic filament system in critical point-dried whole mounts and plastic-embedded sections. *J. Cell Biol.* 100:1474–1487.

Robertson, S., and Potter, J. D. 1984. The regulation of free Ca^{2+} ion concentration by metal chelators. *Methods Pharmacol.* 5:63–75.

Sato, M. W. H., Schwarz, and T. D. Pollard. 1987. Dependence of the mechanical properties of actin/α-actinin gels on deformation rate. *Nature (Lond.).* 325:825–830.

Simon, J. R., and D. L. Taylor. 1986. Preparation of a fluorescent analog: acetamidofluoresceinyl-labeled Dictyostelium discoideum α-actinin. *Methods Enzymol.* 134:487–507.

Simon, J. R., R. H. Furukawa, B. R. Ware, and D. L. Taylor. 1988. The molecular mobility of α-actinin and actin in a reconstituted model of gelation. *Cell Motil. Cytoskeleton.* 11:64–82.

Smith, S. 1988. Neuronal cytomechanics: the actin-based motility of growth cones. *Science (Wash. DC).* 242:708–715.

Stendahl, O., and T. P. Stossel. 1980. Actin-binding protein amplifies actomyosin contraction, and gelsolin confers calcium control on the direction of contraction. *Biochem. Biophys. Res. Commun.* 92:675–681.

Stossel, T. P. 1982. The structure of cortical cytoplasm. *Phil. Trans. Soc. Lond. B.* 299:275–289.

Stossel, T. P. 1990. How cells crawl. *Am. Sci.* 78:408–423.

Stossel, T. P., C. Chaponnier, R. M. Ezzell, J. H. Hartwig, P. A. Janmey, D. J. Kwiatkowski, S. E. Lind, D. B. Smith, F. S. Southwick, H. L. Yin, and K. S. Zaner. 1985. Nonmuscle actin-binding proteins. *Annu. Rev. Cell Biol.* 1:353–402.

Taylor, D. L. 1977. The contractile basis of amoeboid movement. IV. The viscoelasticity and contractility of amoeboid cytoplasm in vivo. *Expt. Cell Res.* 105:413.

Taylor, D. L., and J. S. Condeelis. 1979. Cytoplasmic structure and contractility in amoeboid cells. *Int. Rev. Cytol.* 56:57–143.

Taylor, D. L., and M. Fechheimer. 1982. Cytoplasmic structure and contractility. The solation-contraction coupling hypothesis. *Phil. Trans. Soc. Lond. B.* 299:185–197.

Taylor, D. L., J. S. Condeelis, P. L. Moore, and R. D. Allen. 1973. The contractile basis of amoeboid movement. I. The chemical control of motility in isolated cytoplasm. *J. Cell Biol.* 59:378–394.

Taylor, D. L., Y.-L. Wang, and J. Heiple. 1980*a*. The contractile basis of amoeboid movement. VII. The distribution of fluorescently labeled actin in living amoebae. *J. Cell Biol.* 86:590–598.

Taylor, D. L., J. Blinks, and G. T. Reynolds. 1980*b*. Contractile basis of amoeboid movement. VIII. Aequorin luminescence during amoeboid movement, endocytosis, and capping. *J. Cell Biol.* 86:599–607.

Theriot, J., and T. Mitchison. 1991. Actin microfilament dynamics in locomoting cells. *Nature (Lond.).* 352:126–131.

Tilney, L., and S. Inoue. 1985. Acrosomal reaction of the Thyrone sperm. III. The relationship between actin assembly and water influx during the extension of the acrosomal process. *J. Cell Biol.* 100:1273–1283.

Trinkaus, J. P. 1980. Formulation of protrusions of the cell surface during tissue cell movement. *In* Tumor Cell Surfaces and Malignancy. Alan R. Liss, New York. 887–906.

Wang, Y.-L. 1985. Exchange of actin subunits at the leading edge of living fibroblasts: possible role of treadmilling. *J. Cell Biol.* 101:597–602.

Wang, Y.-L., F. Lanni, P. McNeil, B. Ware, and D. L. Taylor. 1982. Mobility of cytoplasmic and membrane-associated actin in living cells. *Proc. Natl. Acad. Sci. USA.* 79:4660–4664.

Wessels, D., D. Soll, D. Knecht, W. Loomis, A. DeLozzane, and J. Spudich. 1988. Cell motility and chemotaxis in Dictyostelium amoebae lacking myosin heavy chain. *Dev. Biol.* 128:164–177.